

This item is the archived peer-reviewed author-version of:

New error measures for evaluating algorithms that estimate the motion of a range camera

Reference:

Bogaerts Boris, Penne Rudi, Ribbens Bart, Sels Seppe, Vanlanduit Steve.- New error measures for evaluating algorithms that estimate the motion of a range camera
VISIGRAPP 2018 : proceedings of the 13th International Joint Conference on Computer Vision, Imaging and Computer Graphics Theory and Applications : January 27-29, 2018, Funchal, Portugal / Imai, Francisco [edit.] - ISBN 978-989-758-306-3 - Setúbal, Science and Technology Publications, 2018, 5, p. 508-515
Full text (Publisher's DOI): <https://doi.org/10.5220/0006510005080515>
To cite this reference: <https://hdl.handle.net/10067/1535860151162165141>

New error measures for evaluating algorithms that estimate the motion of a range camera

Boris Bogaerts¹, Rudi Penne^{1,2}, Bart Ribbens^{1,3}, Seppe Sels¹ and Steve Vanlanduit¹

¹*Faculty of Applied Engineering, University of Antwerp, Groenenborgerlaan 171, B-2020 Antwerp, Belgium*

²*Department of Mathematics, University of Antwerp, Middelheimlaan 1, B-2020, Belgium*

³*Multimedia and Communication Technology, Karel de Grote University College, Salesianenlaan 90, B-2660 Antwerp, Belgium*

{first_name.family_name}@uantwerpen.be

Keywords: Range camera, Extrinsic calibration, Motion estimation, Conjugacy invariants

Abstract: We compare the classical point-based algorithms for the extrinsic calibration of a range camera to the recent plane-based method. This method does not require any feature detection, and appears to perform well using a small number of planes (minimally 3). In order to evaluate the accuracy of the computed rigid motion we propose two new error metrics that get direct access to the ground truth provided by a mechanism with reliable motion control. Furthermore, these error metrics do not depend on an additional hand-eye calibration between the mechanism and the sensor. By means of our objective measures, we demonstrate that the plane-based method outperforms the point-based methods that operate on 3-D or 2-D point correspondences. In our experiments we used two types of TOF cameras attached to a robot arm, but our evaluation tool applies to other sensors and moving systems.

1 INTRODUCTION

The resolution of most Time-of-Flight (TOF) cameras remains low compared to the resolution of common RGB cameras [Hansard et al., 2012]. This drawback is an obstacle in the detection of point features, which is a bottleneck in many procedures for intrinsic and extrinsic calibration. On the other hand, range cameras provide spatial reconstruction without the need to detect point features. Recent publications demonstrate the advantage of using planes instead of points in the observed scene [Teichman et al., 2013, Penne et al., 2015b, Penne et al., 2015a, Fernández-Moral et al., 2014]. Indeed, planes can be segmented easier than corners can be detected [Fernández-Moral et al., 2014, Penne et al., 2013, Pathak et al., 2010] and they can be reconstructed using robust plane fitters [Torr and Zisserman, 2000].

In this paper we focus on the quality of algorithms for the extrinsic calibration of range cameras, that is, for estimating the rigid transformation between two camera poses given the images of a common scene that are taken from these two poses. We compare three essentially different strategies for obtaining this extrinsic calibration. In the first place, because we use a range sensor, a 3-D point cloud is given in the refer-

ence system of both camera poses. If in addition to the detection of the points in both images also the correspondence between these point images is established, the rigid transformation between these poses can be computed by standard methods as reported in [Eggert et al., 1997] for instance. If the 3-D point clouds in the two camera reference systems are given without correspondences, an iterative closest point algorithm can be applied (as coined in [Besl and McKay, 1992]), at the cost of accuracy [Bellekens et al., 2015]. On the other hand, a TOF camera (the range sensor that is used in our experiments) also provides a 2-D intensity image. If planar calibration patterns such as checker boards are viewed by both camera poses, the transformation of these boards relative to each camera pose can be computed by classical calibration procedures [Zhang, 2000, Zhang, 1989]. Consequently, this yields the relative rigid transformation between both camera poses. Last but not least, the arguments listed in the previous paragraph suggest to use flat objects (planes) rather than points. As a matter of fact, this option is preferred in several publications, e.g. in the extrinsic calibration procedure of [Fernández-Moral et al., 2014] or in the registration algorithm of [Pathak et al., 2010]. In Section 2.3, we describe and explain this plane-based method via an elemen-

tary route, using the dual projective transformation (in the same spirit as [Vasconcelos et al., 2012, Raposo et al., 2013]). Other remarkable methods for extrinsic calibration that offer alternatives to point measurements can be found in [Guan et al., 2015] (for RGB-cameras, by means of spheres) or in [Sabata and Aggarwal, 1991] (for range sensors, using lines or surfaces). But for reasons listed above, we prefer a motion-from-planes approach.

The first contribution of this paper is to prove that the computation of the rigid motion between two poses of a TOF camera is more accurate and more robust when the range data is used, rather than the luminance data. Although this conclusion could have been predicted, it is comforting to confirm it by a scientific procedure, because the sources and the propagation of errors are not the same for the 2D-sensor as for the range sensor. In addition, we will conclude that the estimated motion computed by the plane-based method is more accurate than the point-based method (Section 5), even when only a few planes are available in the common view area (three, at most four). For this comparative study we used an implementation of the SVD algorithm of [Arun et al., 1987] for the 3-D point-based method, an implementation of [Zhang, 1989] for the 2-D point-based method and in essence the algorithm of [Fernández-Moral et al., 2014] for the 3-D plane-based method.

The second (and to our opinion the most important) contribution of this paper is the proposal of a new type of error measures that directly refer to an absolute ground truth for the estimated rigid motion. So far, research articles evaluated the computed extrinsic calibration indirectly because the ground truth for camera motion seemed inaccessible. Common performance measures for extrinsic calibration in the absence of ground truth are the triangulation error, the projection error or the reprojection error [Guan et al., 2015]. Unfortunately, these error measures need data consisting of points and hence are not suitable to validate a plane-based method. Furthermore, they implicitly evaluate the intrinsic calibration of the used camera(s) as well. Sometimes, the rigid transformation supplied by a state-of-the-art method such as [Tsai, 1992] is used as ground truth, e.g. in [Guan et al., 2016], which cannot be considered as absolute reference either. In our experiments, the TOF camera was rigidly attached to a robot manipulator (Fig. 1). The motion of the robot’s end effector can be considered as a very accurate ground truth.

However, it is a challenge to have access to this ground truth data, because of the famous hand-eye calibration problem [Shah et al., 2012]. This problem is caused by the fact that the relative motion be-

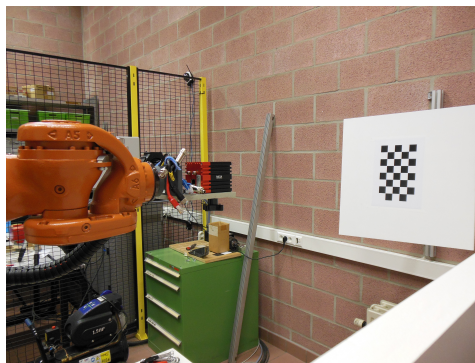


Figure 1: We controlled the motion of a TOF camera by attaching it to an articulated robotarm.

tween two positions of the camera is known in the robot basis instead of the camera basis. The transformation matrix between both reference frames, one at the camera center and the other at the robot tool center, is an obstacle to get access to the ground truth provided by the robot motion. We can solve for this transformation matrix by doing the hand-eye calibration [Mao et al., 2010, Shah et al., 2012], but this is based on the availability of a reliable camera transformation. Therefore, using the hand-eye calibration for evaluating the extrinsic calibration (camera motion) gives rise to a conceptual loop, and hence is not desirable. Therefore, we propose to use algebraic conjugacy invariants, and introduce two new error metrics. A major drawback of our approach is the lack of physical interpretation of these error measures because they have an algebraic rather than a geometric nature. However, they provide a correct scale to compare different methods. As a matter of fact, it can be used to compare all algorithms for extrinsic calibration, as long as the involved sensor can be attached to mechanism with precisely controllable motions. The reason why we develop more than one error metric is the fact that there does not exist a standard procedure yet to validate camera motion by means of robot motion. Fortunately, the results by both metrics correlate, providing convincing proof for the ranking of the three considered methods.

The paper is organized as follows. In Section 2 we give an overview of the three methods that we will evaluate for estimating the rigid motion of a TOF camera. In Section 3 we explain our error metrics for validating the computed camera motion by means of the given robot motions, taking into account that the hand-eye transformation X is unknown to us. Section 4 describes the details of the setup of the experiments. Section 5 contains the results of the evaluation of the three compared methods, for two types of TOF cameras, by means of the proposed error metrics.

2 RIGID CAMERA MOTION: DESCRIPTION OF THREE METHODS

A common way to describe mathematically the rigid motion of a TOF camera or any other 3-D object is by means of the coordinate transformation between the two positions of a rigidly attached reference frame before and after the motion. The rotational part of the rigid motion is represented by a 3×3 orthonormal matrix R ($R^{-1} = R^T$), and the translation part by a 3×1 vector t . If p and p' are the 3×1 coordinate vectors of a given spatial point w.r.t. the rigidly attached reference frame before and after the motion respectively, then

$$p = R \cdot p' + t. \quad (1)$$

Often, it is convenient to represent this transformation by one matrix multiplication $\bar{p} = B \cdot \bar{p}'$, using homogeneous coordinates $\bar{p} = (p^T, 1)^T$ with weight 1, and a 4×4 transformation matrix

$$B = \begin{pmatrix} R & t \\ \mathbf{0}^T & 1 \end{pmatrix} \quad (2)$$

with $\mathbf{0}$ the 3×1 zero vector.

In this section we exhibit three essentially different methods for estimating the rigid motion of a TOF camera.

2.1 2-D extrinsic calibration

In the first method we do not use the depth measurements of the involved range sensor, but only its luminance image (2-D intensity image). Estimating the motion between two camera positions is equivalent to a stereo calibration from two 2-D-images, and can be done by proven procedures, e.g. as described in [Zhang, 1989]. In our experiments, we carefully accomplished a lateral calibration of the TOF camera, that is, we determined the intrinsic pinhole parameters and removed non-linear lens distortion in a pre-processing step.

Next, for each camera position we computed the 4×4 rigid transformation matrix H with respect to a fixed calibration checkerboard with known size (Section 4). Finally, the extrinsic transformations H_1 and H_2 of both camera positions relative to the fixed calibration pattern yield the rigid transformation $B = H_2^{-1} \cdot H_1$ of the camera.

2.2 3-D point measurements

Given a set of corresponding 3-D points,

$$p_1, \dots, p_N \longleftrightarrow p'_1, \dots, p'_N \quad (3)$$

there are several methods to estimate the rigid transformation (R, t) mapping the first set to the second. A comparison between different methods is presented in the review paper [Eggert et al., 1997]. The determination of the most likely translation t and rotation R comes down to finding the least-squares solution of a system of $3N$ linear equations caused by N pairs of corresponding 3-D points, where each pair yields 3 equations as given by Eqn. 1. Equivalently, the motion pair (R, t) is determined by minimizing the sum of squares error:

$$SSE = \sum_{i=1}^N \|p_i - R p'_i - t\|^2 \quad (4)$$

subject to the constraint that R has to be orthonormal. In our experiments we followed the method of [Arun et al., 1987], that computes the rotation and translation separately. As a first step this centroid is calculated both before and after transformation, p_c and p'_c , such that both point clouds can be presented relative to their centroid: $p_{ci} = p_i - p_c$ and $p'_{ci} = p'_i - p'_c$. In [Arun et al., 1987] it is proved that the rotation matrix R that minimizes SSE is given by

$$R = V U^T, \quad (5)$$

where the matrices V and U are found by the singular value decomposition $H = U \Lambda V^T$ of

$$H = \sum_{i=1}^N p'_{ci} p_{ci}^T. \quad (6)$$

Finally, the translation part is estimated by means of both centroids: $t = p_c - p'_c$.

2.3 3-D plane measurements

If the rigid transformation of a depth camera is represented by a 4 by 4 transformation matrix B acting on homogeneous coordinates of 3-D points as given by Eqn. 2, then the corresponding dual transformation acting on plane coordinates $(a, b, c, d)^T$ is represented by B^{-T} [Pottmann and Wallner, 2001]:

$$\begin{pmatrix} a \\ b \\ c \\ d \end{pmatrix} \sim B^{-T} \begin{pmatrix} a' \\ b' \\ c' \\ d' \end{pmatrix} \Leftrightarrow \begin{pmatrix} a' \\ b' \\ c' \\ d' \end{pmatrix} \sim B^T \begin{pmatrix} a \\ b \\ c \\ d \end{pmatrix} \quad (7)$$

Because the homogeneous plane coordinates $(a, b, c, d)^T$ are determined up to a scale factor, it is convenient to normalize the plane normals $n = (a, b, c)^T$ to length 1. This leaves us with one more ambiguity, due to the two opposite directions for n . This can be resolved by some additional constraint, e.g. requiring that all plane normals point

towards the 3D sensor. With these conventions the proportional similarity of Eqn. 7 can be replaced by an equality. Consequently, the rigid motion (R, t) of the camera transforms the plane coordinates $(n^T, d)^T$ for k considered planes as follows:

$$\begin{aligned} \begin{pmatrix} n'_1 & \dots & n'_k \\ d'_1 & \dots & d'_k \end{pmatrix} &= \begin{pmatrix} R^T & 0 \\ t^T & 1 \end{pmatrix} \begin{pmatrix} n_1 & \dots & n_k \\ d_1 & \dots & d_k \end{pmatrix} \\ &= \begin{pmatrix} R^T n_1 & \dots & R^T n_k \\ t^T \cdot n_1 + d_1 & \dots & t^T \cdot n_k + d_k \end{pmatrix} \end{aligned} \quad (8)$$

These equations can be decoupled into a system for R and a system of t . Furthermore, the equations for R make only use of the plane normals:

$$\begin{aligned} (n'_1 \dots n'_p) &= R^T (n_1 \dots n_p) \\ (d'_1 \dots d'_p) &= t^T (n_1 \dots n_p) + (d_1 \dots d_p) \end{aligned} \quad (9)$$

So, the rotational part of the desired rigid motion can be estimated by minimizing

$$SSE = \sum_{i=1}^p \|n_i - Rn'_i\|^2 \quad (10)$$

in the same spirit of [Arun et al., 1987]. This is equivalent to maximizing $\text{trace}(RH)$, where H is the 3×3 matrix defined by

$$H = \sum_{i=1}^p n'_i n_i^T, \quad (11)$$

which is accomplished once again by the SVD $H = U\Lambda V^T$ and putting $R = VU^T$. On the other hand, the translational part t can be estimated by a least squares solution for the equations containing t in the system of Eqn. 9.

3 ERROR METRICS

3.1 The charpoly error metric

In our experiments we have used two error metrics in order to evaluate the accuracy of different methods for estimating the rigid camera motion. The validation is done by means of the known motion of an articulated robot arm where the camera was rigidly attached to (Fig. 1). Therefore, we introduce error metrics that leverage the fact that the camera motion is *conjugated* to the known robot motion. This means that the motion is the same, but expressed in different bases. If the 4×4 transformation matrix A denotes the motion of the robot, and if B represents the camera motion matrix, then this conjugacy is algebraically expressed by *similarity* of matrices [Hoffman and Kunze, 1971]:

$$A = XB X^{-1} \quad (12)$$

In the literature this issue is also known as the $AX = XB$ calibration problem [Mao et al., 2010]. This 4×4 matrix X is the so-called *hand-eye calibration* between robot and camera. In general, the transformation X between the robot coordinate frame and the camera frame is not a priori known. In our validation experiments, the robot transformation A is accurately known and considered as ground truth, while the estimation of B using different algorithms has to be validated.

In order to validate B by means of A we can use conjugacy invariants. It is a fundamental algebraic property that similar matrices have the same characteristic polynomial [Hoffman and Kunze, 1971]:

$$p(\lambda) = \det(A - I_4\lambda) = \det(B - I_4\lambda) \quad (13)$$

Each coefficient of this characteristic polynomials can serve to evaluate camera motion matrices against the known robotic motion matrices. In theory these coefficients are identical. A 4×4 transformation matrix has a characteristic polynomial of degree 4 with five coefficients:

$$\begin{aligned} p(\lambda) &= \lambda^4 + (\text{tr}(R) - 1)\lambda^3 - (\text{tr}(R) + k)\lambda^2 \\ &\quad + (k - \det(R))\lambda + \det(R) \end{aligned} \quad (14)$$

Analyzing the calculation of the characteristic equation of a rigid transformation matrix reveals that two parameters determine all the coefficients. The first parameter is the trace of the rotational part R of the transformation matrix. The second parameter (k) is a bit more complicated:

$$k = r_{11}r_{22} + r_{11}r_{33} + r_{22}r_{33} + r_{31}r_{13} + r_{23}r_{32} + r_{12}r_{21} \quad (15)$$

This parameter k and the trace of the rotational part are the two components that compose the first error metric that we suggest, the *charpoly error metric*. Notice that this error metric only provides a quality evaluation for the rotational part of the calculated transformation matrix.

$$CPE_{\text{tr}} = \text{tr}(R_A) - \text{tr}(R_B) \quad (16)$$

$$CPE_k = k_A - k_B \quad (17)$$

These two parameters will be kept separate because it is not immediately obvious how to combine them into one parameter that describes the global similarity between matrices A and B .

3.2 The hand-eye error metric

The second error metric that we propose is less straightforward. In this metric different measurements associated with several camera transformations

will be combined in a system of equations that could be used to compute the hand-eye calibration X :

$$AX - XB = 0 \quad (18)$$

These matrices are all 4×4 transformation matrices and can be expressed as block matrices:

$$\begin{pmatrix} R_A & t_A \\ \mathbf{0}^T & 1 \end{pmatrix} \begin{pmatrix} R_X & t_X \\ \mathbf{0}^T & 1 \end{pmatrix} = \begin{pmatrix} R_X & t_X \\ \mathbf{0}^T & 1 \end{pmatrix} \begin{pmatrix} R_B & t_B \\ \mathbf{0}^T & 1 \end{pmatrix}. \quad (19)$$

Or, after performing the matrix multiplications:

$$\begin{pmatrix} R_A R_X & R_A t_X + t_A \\ \mathbf{0}^T & 1 \end{pmatrix} = \begin{pmatrix} R_X R_B & R_X t_B + t_X \\ \mathbf{0}^T & 1 \end{pmatrix}. \quad (20)$$

Using the *tensor product* \otimes of matrices and the *vectorization* $\text{vec}(Q)$ denotes of matrix Q , we obtain a system of 12 linear equations in the 9 unknowns $(\text{vec}(R_X)^T, t_X^T)$ [Petersen and Pedersen, 2012]:

$$\underbrace{\begin{pmatrix} I_3 \otimes R_A - R_B^T \otimes I_3 & 0 \\ t_B^T \otimes I_3 & I_3 - R_A \end{pmatrix}}_M \begin{pmatrix} \text{vec}(R_X) \\ t_X \end{pmatrix} = \underbrace{\begin{pmatrix} \mathbf{0} \\ t_A \end{pmatrix}}_s \quad (21)$$

Eqn. 21 was mentioned in the review paper [Shah et al., 2012] on hand-eye calibration. In order to determine (R_X, t_X) we need to know the robot motion A and the corresponding measured camera transformation B . To actually solve this system, at least three given transformation pairs (A, B) are necessary. In practice, coping with noisy measurements, we combine Eqn. 21 for multiple transformation pairs $(n \geq 3)$ as follows:

$$\begin{pmatrix} M_1 \\ \vdots \\ M_n \end{pmatrix} \begin{pmatrix} \text{vec}(R_X) \\ t_X \end{pmatrix} = \begin{pmatrix} s_1 \\ \vdots \\ s_n \end{pmatrix} \quad (22)$$

Now we introduce our second error metric, as a quality measure of the system in Eqn. 22. It is the mean residue for the least squares solution to the transformation X :

$$HEE = \sqrt{\|s - M(M^T M)^{-1} M^T s\|^2 / (12n)} \quad (23)$$

with $M = (M_1^T, \dots, M_n^T)^T$ and $s = (s_1^T, \dots, s_n^T)^T$. We refer to this error metric with the acronym *HEE* (hand-eye-error). The error metric provided by Eqn. 23 is motivated by the following arguments:

- The robot transformation A is known accurately.
- The transformation matrix X necessarily exists and is fixed for a given robot-sensor system. Therefore *HEE* would be 0 if the rigid motion B of the depth sensor was computed correctly (assuming zero noise for A).
- *HEE* is able to assess the validity of a method over multiple measurements, yielding a growing system of equations (Eqn. 22). Therefore, it also evaluates the stability of a proposed method.

4 EXPERIMENTAL SETUP

The objective of our experiments is to evaluate the accuracy of three different methods for computing the rigid motion of a TOF camera. All the tests have been repeated for two common Time-of-Flight cameras: **Kinect V2** and **Mesa SR4000**. In order to compare the computed motion to a reliable ground truth, the Time-of-Flight sensors are mounted rigidly on an articulated robotarm (KUKA KR16, with a repeatability error less than 0.1mm). See Fig. 1. In each single test we consider TOF images for a pair of robot positions, in which the attached camera observes a classical calibration checkerboard. During the whole experiment we arranged 6 distinct positions of this checkerboard, that could be viewed from 20 pre-programmed robot configurations, providing a supply of $6 \times \binom{20}{2}$ test pairs for each camera.

The detection of the checker corners is performed in the luminance images of the TOF cameras. For the 2-D extrinsic calibration we used an implementation of [Zhang, 2000], combined with a nonlinear optimization to minimize the reprojection error.

For the second and third method we needed a set of 3-D points, generated by both used types of TOF sensors, directly provided in (X, Y, Z) coordinates with respect to the camera frame. This means that we assumed a priori calibrated TOF cameras. The 3-D point-based method makes use of pairs of corresponding points in both range sensors. Because TOF cameras deliver poor depth measurement accuracy at the detected checker corners due to the black-white transitions [Pattinson, 2011, Fuchs and May, 2008], we preferred to reconstruct the centers of the white checkerboard. These centers can be found by intersecting the diagonals of the checker squares. Note however that these square centers (nor the checker corners) are likely to coincide with a pixel, causing additional round off errors for the depth measurements.

The third method, based on plane measurements, is by far the most user friendly one. Here there is no need for performing feature detection and find point correspondences. We only reconstruct points on the plane supporting the checker board. To this end we automatically selected the pixels in the white checkers and on the larger panel that the calibration board had been attached to. The 3-D measurements are directly available in these pixels, avoiding depth interpolation. Furthermore, depth measurements for white pixels are known to be more accurate than for black pixels [Pattinson, 2011, Fuchs and May, 2008]. Next, we compute the best-fitting plane supporting the reconstructed 3-D points in each of both given range im-

ages of a fixed calibration board. Working with these plane coordinates flattens error fluctuations for the 3-D point measurements, and moreover avoids the task to detect features and to establish correspondences. This best-fitting plane can be computed by *principal component analysis*, but we prefer a more robust estimate based on Ransac [Fischler and Bolles, 1981]. More precisely, we applied an implementation of the algorithm of [Torr and Zisserman, 2000].

5 RESULTS

For the sake of validation, random transformations are sampled from our dataset. This dataset consists of measurements from 20 different robot positions (Section 4). In each such position, 6 images have been taken by a TOF sensor that was rigidly attached to the articulated robot arm. These TOF images contain both 2-D intensity images and depth measurements of the 6 fixed spatial positions of a calibration checkerboard. Finally, all these measurements have been repeated for two different commonly used Time-of-Flight cameras: Kinect V2 and Mesa SR4000. For the three methods that we intend to evaluate, the rigid camera motion is estimated for some randomly selected pairs of robot positions. The three algorithms always operate on the same pairs of robot positions for the sake of comparison.

1. For the first method, the extrinsic calibration based on the 2-D luminance images, we use one randomly selected calibration plane image, the same for both robot positions. The checker corners are detected at subpixel level, the correspondence is established in the pair of 2-D images, and the relative transformation between both camera poses is estimated via two extrinsic calibrations relative to the calibration plane position.
2. If the rigid transformation is estimated by means of 3-D point correspondences, the same calibration plane is used. The depth images enable spatial recoveries of the white square midpoints (intersection of the diagonals), providing a corresponding pair of 3-D point sets.
3. In case we compute the rigid camera motion (R, t) by means of planes as a solution of the system given by Eqn. 9, some fixed number of planes are randomly selected from the 6 available calibration boards. A solution of the system given by Eqn. 9 is determined if at least three planes with linearly independent normals are available.

5.1 Evaluation by means of the charpoly error metric

In our experiment a large amount of transformations are sampled from the total set of possible transformations in the constructed dataset. The calculated transformations are compared to the ground truth robot motion. To accomplish this goal we can use the algebraic conjugacy invariants of Section 3.1. The absolute difference between both traces of the rotational part and the defined k value are stored. To evaluate the quality of the rotational part of the obtained transformation the distributions of the charpoly error metric are visualized using boxplots (Fig. 2). For both cameras we observe that the two conjugacy invariants constituting the charpoly error metric (trace and k) agree in their evaluation.

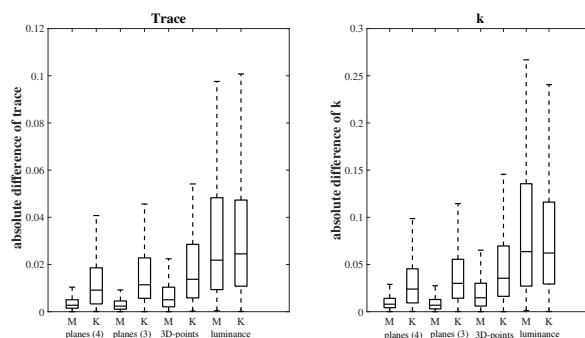


Figure 2: The quality of the rotation between two positions of TOF camera is compared for the three described methods. The plane-based method was done for 3 and for 4 planes. The two parameters of the charpoly error metric are evaluated for the Kinect V2 (K) and the Mesa SR4000 (M).

The quality of the estimated rotation as obtained by the plane-based method is similar to the rotation as obtained by 3-D points, as far as the charpoly error metric is concerned (Fig. 2). Next, it is striking that the 3-D methods (operating on range data) compute the camera rotation with a lower median error value and smaller spread than the 2-D method (operating on luminance images). So, it appears that the 2-D method for extrinsic calibration of a 3-D sensor is less accurate and less robust.

We also observe that the plane method performs very well even when using the required minimum of 3 planes, and only slightly better when using 4 planes. Our experiments demonstrate that using more redundancy (5 or 6 planes) does not imply a better quality of the estimated transformation. The empirical fact that estimating a camera motion by means of 3 or 4 planes is at least as good as by means of 20 correspondence pairs of 3-D points, and definitely better than by 2-D

extrinsic calibration, can be explained by the fact that the involved plane normals are very reliable. They are obtained by a robust plane fitter, averaging out occurring depth noise.

5.2 Evaluation by means of the hand-eye error metric

In this validation a fixed number of transformations (pairs of robot positions) were sampled for each hand-eye calibration system size.

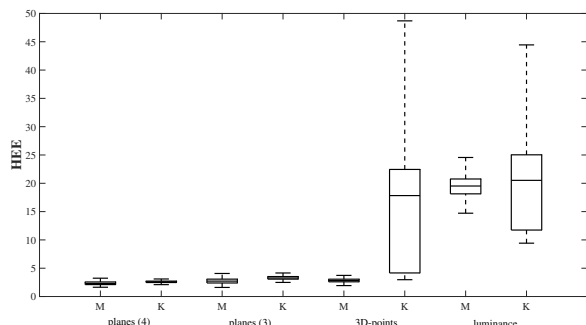


Figure 3: A boxplot visualizing the distribution of the hand-eye error for the evaluated methods, for the Mesa SR4000 (M) and for the Kinect V2 (K). Methods with a very broad distribution are unstable and thus unreliable.

During the experiment it turned out that the magnitude of the hand-eye error strongly depends on the selected transformation. However, this ‘instability problem’ was not observed for the plane-based method, for none of the used cameras (Fig. 3). The evaluation by the hand-eye error metric implies that the point-based methods are inherently too inconsistent to compute the hand-eye calibration between robot and camera, while the plane-based method appears to be able to estimate a hand-eye transformation in a consistent way, independent of the considered robot configurations. The inferior result of the 3-D point method for the Kinect camera can be explained by its larger field of view compared to that of the Mesa camera. Consequently, the working distance of the Kinect is larger, and therefore the image size of the checkerboard is smaller than observed by the Mesa. This results in a bigger round of error in the point matching. This inherent drawback for the 3-D point method is circumvented by the 3-D plane method.

6 CONCLUSIONS

We investigated the quality of several methods for computing of the rigid motion of a TOF camera. We

evaluated the classical 2-D stereovision approach, using only the luminance images of the TOF camera, and two 3-D methods that take benefit from the range data. The 3-D points method needs corner detection and point correspondences, while for the 3-D planes method we only have to randomly select pixels in a segmented region. In our experiments we considered the motion of a computer driven robot arm as ground truth. In order to have access to this ground truth and to get around the unknown hand-eye transformation, we designed two error metrics, being algebraic conjugacy invariants. We believe that our evaluation for extrinsic calibration methods is more appropriate than other performance measures such as triangulation error or reprojection error, because we do not depend on feature detection nor correspondence determination. Furthermore, the ground truth provided by a robot manipulator is more absolute and reliable compared to a reference obtained from a state-of-the-art algorithm. All our experiments, for both types of cameras and for both proposed error measures, agreed on the same conclusions:

- The 3-D methods for estimating the motion of a range camera definitely outperform 2-D methods.
- The 3-D planes method appears to be more robust and accurate than the 3-D points method.
- it appears that only a small number of planes (3 or 4) are needed to guarantee the reported for the plane-based method.

Acknowledgements

The first author holds a PhD grant from the research Fund-Flanders (FWO Vlaanderen).

REFERENCES

- Arun, K. S., Huang, T. S., and Blostein, S. D. (1987). Least-squares fitting of two 3-d point sets. *9(5):698–700*.
- Bellekens, B., Spruyt, V., Berkvens, R., Penne, R., and Weyn, M. (2015). A benchmark survey of rigid 3d point cloud registration algorithms. *Int. J. Adv. Int. Systems*, 8(1 & 2):118–127.
- Besl, P. J. and McKay, N. D. (1992). A method for registration of 3-d shapes. *IEEE Trans. Pattern Anal. Mach. Intell.*, 14(2):239–256.
- Eggert, D., Lorusso, A., and Fisher, R. (1997). Estimating 3-d rigid body transformations: a comparison of four major algorithms. *Machine Vision and Applications*, 9(5):272–290.

- Fernández-Moral, E., González-Jiménez, J., Rives, P., and Arévalo, V. (2014). Extrinsic calibration of a set of range cameras in 5 seconds without pattern. In *International Conference on Intelligent Robots and Systems*. IEEE/RSJ.
- Fischler, M. and Bolles, R. (1981). Random sampling consensus: A paradigm for model fitting with applications to image analysis and automated cartography. *Communications of the ACM*, 24:381–385.
- Fuchs, S. and May, S. (2008). Calibration and registration for precise surface reconstruction with time of flight cameras. *Int. J. Intell. Syst. Technol. Appl.*, 5(3/4):274–284.
- Guan, J., Deboeverie, F., Slembrouck, M., van Haerenborgh, D., van Cauwelaert, D., Veelaert, P., and Philips, W. (2015). Extrinsic calibration of camera networks using a sphere. *Sensors*, 15(8):18985–19005.
- Guan, J., Deboeverie, F., Slembrouck, M., Van Haerenborgh, D., Van Cauwelaert, D., Veelaert, P., and Philips, W. (2016). Extrinsic calibration of camera networks based on pedestrians. *Sensors*, 16(5).
- Hansard, M., Lee, S., Choi, O., and Horaud, R. (2012). *Time of Flight Cameras: Principles, Methods, and Applications*. SpringerBriefs in Computer Science. Springer.
- Hoffman, K. and Kunze, R. (1971). *Linear algebra*. Prentice-Hall mathematics series. Prentice-Hall.
- Mao, J., Huang, X., and Jiang, L. (2010). A flexible solution to $ax=xb$ for robot hand-eye calibration. In *Proceedings of the 10th WSEAS International Conference on Robotics, Control and Manufacturing Technology*, ROCOM'10, pages 118–122, Stevens Point, Wisconsin, USA. World Scientific and Engineering Academy and Society (WSEAS).
- Pathak, K., Birk, A., Vaškevičius, N., and Poppinga, J. (2010). Fast registration based on noisy planes with unknown correspondences for 3-d mapping. *Trans. Rob.*, 26(3):424–441.
- Pattinson, T. (2011). *Quantification and Description of Distance Measurement Errors of a Time-of-Flight Camera*. PhD thesis, University of Stuttgart.
- Penne, R., Mertens, L., and Ribbens, B. (2013). Planar segmentation by time-of-flight cameras. In *Advanced Concepts for Intelligent Vision Systems*, volume 8192 of *Lecture Notes in Computer Science*, pages 286–297.
- Penne, R., Raposo, C., Mertens, L., Ribbens, B., and Araujo, H. (2015a). Investigating new calibration methods without feature detection for tof cameras. *Image and Vision Computing*, 43:5062.
- Penne, R., Ribbens, B., and Mertens, L. (2015b). An incremental procedure for the lateral calibration of a time-of-flight camera by one image of a flat surface. *International Journal of Computer Vision*, 113(2):81–91.
- Petersen, K. B. and Pedersen, M. S. (2012). *The Matrix Cookbook*. Technical University of Denmark. Version 20121115.
- Pottmann, H. and Wallner, J. (2001). *Computational Line Geometry*. Springer-Verlag New York, Inc., Secaucus, NJ, USA.
- Raposo, C., Barreto, J., and Nunes, U. (2013). Fast and accurate calibration of a kinect sensor. In *International Conference on 3D Vision*. IEEE.
- Sabata, B. and Aggarwal, J. (1991). Estimation of motion from a pair of range images: A review. *CVGIP: Image Understanding*, 54(3):309 – 324.
- Shah, M., Eastman, R. D., and Hong, T. (2012). An overview of robot-sensor calibration methods for evaluation of perception systems. In *Proceedings of the Workshop on Performance Metrics for Intelligent Systems*, PerMIS '12, pages 15–20, New York, NY, USA. ACM.
- Teichman, A., Miller, S., and Thrun, S. (2013). Unsupervised intrinsic calibration of depth sensors via SLAM. In *Robotics: Science and Systems*.
- Torr, P. and Zisserman, A. (2000). Mlesac: A new robust estimator with application to estimating image geometry. *Comput. Vis. Image Underst.*, 78(1):138–156.
- Tsai, R. Y. (1992). Radiometry. chapter A Versatile Camera Calibration Technique for High-accuracy 3D Machine Vision Metrology Using Off-the-shelf TV Cameras and Lenses, pages 221–244. Jones and Bartlett Publishers, Inc., USA.
- Vasconcelos, F., Barreto, J., and Nunes, U. (2012). A minimal solution for the extrinsic calibration of a camera and a laser-range-finder. *IEEE Trans Pattern Anal Mach Intell.*, 34(11):2097–2107.
- Zhang, Z. (1989). Motion and structure from two perspective views: algorithms, error analysis, and error estimation. 11(5):451–476.
- Zhang, Z. (2000). A flexible new technique for camera calibration. 22(11):1330–1334.